

# Capítulo 10

## TEMPERATURE FIELD FORECAST IN CONCRETE DAM WITH THE USE OF ARIMA MODELS AND THE FINITE ELEMENT METHOD

*Tásia Hickmann*

*Luiz Albino Teixeira Júnior*

*Alvaro Eduardo Faria*

*Samuel Bellido Rodrigues*

*Jairo Marlon Côrrea*

*Everton Luís Garcia*

**Resumo:** Este artigo descreve um método de previsão, com a aplicação de modelos estatísticos Auto-Regressivo Integrado Média Móvel (ARIMA) e um modelo de condução de calor para prever o campo de temperatura em um bloco de contraforte da barragem de Itaipu. As séries de temperatura mensais de 2010-2014 dos termômetros da superfície ao bloco foram ajustadas por meio de splines cúbicas e a séries, agora diárias, foram utilizadas como entradas para modelos específicos ARIMA para produzir previsões como saídas. Estas saídas foram utilizadas como condições de contorno para o modelo térmico do bloco e este resolvido pelo Método dos Elementos Finitos (MEF). Obtidos assim os campos de temperatura previstos do bloco. O erro MAPE entre os valores obtidos pelo MEF e o real, em um ponto de prova, (onde está um termômetro interno) mediu o desempenho da previsão dos modelos ARIMA, e este foi satisfatório, alcançando valor próximo a 15%. O método proposto tem um caráter inovador para estruturas de análise térmica, em particular em barragens de concreto.

**Palavras-Chave.** Equação do Calor, Séries Temporais, métodos aproximados.

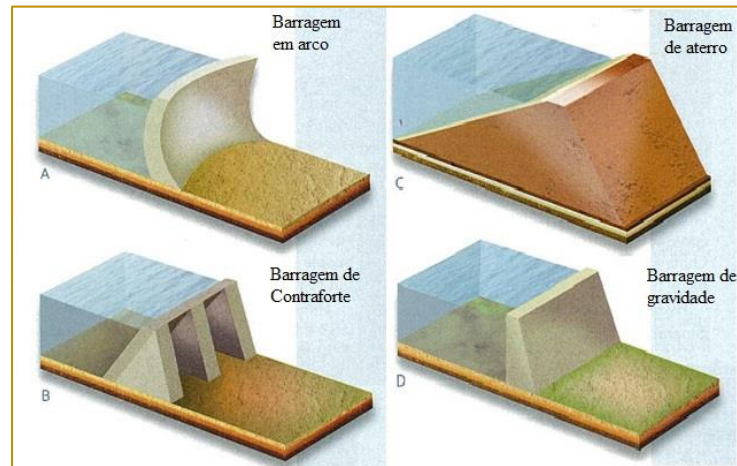
\*Artigo originalmente apresentado no Simpósio Brasileiro de Pesquisa Operacional (SBPO 2016)

## 1. INTRODUCTION

Dams are hydraulic structures built in the course of a river to create a reservoir on its upstream side for the abstraction of water to be used in irrigation, water supply, flood control, navigation, fishing or hydroelectricity production. Dams built for hydroelectricity generation can be classified into two large

groups according to the types of material used in their construction, namely (i) concrete dams, such as gravity arches or buttresses, or (ii) conventional land and rock fill dams. The dam drawings in Figure 1A, 1B and 1D illustrate concrete dams and while the one in Figure 1C illustrates a conventional land and rock fill dam.

Figure 1. Types of dams according to the material used.



Source: Adapted from AUSTRALIAN GEOGRAPHIC

According to [Maken et al. 2013] dams are subject to changes in internal temperature due to external temperature changes and hydration heat (a heat source from concrete chemical reactions during the dam construction but which dissipates in time). The external heat load to a dam surface originates from solar radiation as well as from air, foundation and reservoir temperature variations. Those external heat loads can cause serious physical deformations and significant volumetric changes in the dam structure that often exceed the tensile strength of concrete leading to the development of cracks. Therefore the monitoring of external sources of temperature is crucial for dam structural safety. In fact, a correct evaluation of the temperature field in the dam is essential for determining stresses and deformations of thermal origin. In this regard, predictions of the temperature field are necessary for monitoring and predicting deformations in the dam structure. In this paper, statistical forecasting methods are devised to produce reliable systematic predictions of that temperature field.

To help assess the risk of dam deformation of thermal origin, we have formulated and

applied time series forecasting models to the temperatures recorded by thermometers placed in a buttress dam block of the Itaipu Hydroelectric Power Plant (IHPP) during operational phase. Since these thermometers have only monthly readings, set initially to cubic splines interpolating data to obtain daily data, needed to solve the thermal block model. With these new series, applied Auto-Regressive Integrated Moving Average (ARIMA) forecasting models and the temperature forecasts produced by those models were used as boundary conditions in a thermal model represented by a heat conduction equation for the block. The thermal model in turn was solved by the Finite Element Method (FEM) with the aid of ANSYS simulation software to model the temperature field in the block during the forecasting period.

There is a body of literature covering methods to describe the temperature field in concrete dams through the FEM. In [Daoud et al. 1997], for example, a numerical evaluation of the periodic temperature field in a concrete dam was performed that accounted for ambient temperature changes, solar radiation, snow

cover, temperature gradients and ice formation in reservoir water.

Mirzabozorg et al. 2014] investigated the effects of solar radiation on the thermal distribution on a dam arc and compared the results with those obtained from data recorded from the dam site. The development of [Noorzaei et al. 2006] focused on implementing and verifying a two-dimensional finite element code developed for thermal and structural analysis of Kinta gravity dam in Malaysia, during its construction. Local climatic conditions and thermal properties of materials were considered in the analysis. The temperatures provided by their approximate method were considered in good agreement with the actual temperatures measured by thermocouples installed in the dam body.

For applications of the ANSYS simulation software in engineering problems, particularly in thermal structure analysis, please refers to [Moaveni 2008] and [Madenci and Guven 2015].

Despite the above mentioned contributions to the literature on the thermal modelling of concrete dams, we notice the lack of research related to the forecasting analysis of dam temperature field during operational phase. With observed data from thermometers installed in concrete, the use of statistical forecasting ARIMA models of [Box and Jenkins 1970] and the FEM method (see e.g. [Madenci and Guven 2015]) for heat diffusion models to characterize the evolution of the temperature field in the dam in a future period is feasible. Therefore, prediction of the thermo-structural behavior of the dam can be investigated so that intervention in the structure may be taken, if necessary.

The mathematical modeling of conductive heat transfer process, the characterization of

FEM in the Galerkin method for solving the thermal model, the statistical forecasting of temperature from thermometers installed on the surface of a buttress concrete block of a dam and the forecast of temperature fields in this block are the objectives of this work.

This paper is structured as follows: Section 2 reviews the technical literature associated with the models that compound the proposed thermal forecasting method. It describes the heat conduction equation with the initial and boundary conditions necessary for obtaining its solution and an approximate method for solving the thermal model (the FEM) as well as the statistical forecasting ARIMA model. Section 3 describes the proposed methodology and its application to a case study of the IHPP dam. Predictions of the temperature field of a block of concrete in the dam is obtained by the method and its performance is evaluated. Section 4 concludes the paper.

## 2. ORIENTED LITERATURE REVIEW

### 2.1. HEAT CONDUCTION EQUATION

Conduction heat transfer aims to determine the temperature field of a medium resulting from conditions imposed on its borders. The classical equation for heat diffusion is determined by the first law of thermodynamics and by the Fourier law. It is an empirical relationship involving the heat flow and the temperature gradient through a proportionality constant called the thermal conductivity of the properties materials.

According to [Ozisik 1993], the heat conduction equation for an anisotropic material is given by:

$$\frac{\partial}{\partial x} \left( k_x(T) \frac{\partial T}{\partial x} \right) + \frac{\partial}{\partial y} \left( k_y(T) \frac{\partial T}{\partial y} \right) + \frac{\partial}{\partial z} \left( k_z(T) \frac{\partial T}{\partial z} \right) + G = \rho c \frac{\partial T}{\partial t}, \quad (1)$$

where  $k_x(T)$ ,  $k_y(T)$  and  $k_z(T)$  are the thermal conductivities ( $W/mK$ ) dependent on the temperature in the directions  $x$ ,  $y$  and  $z$ , respectively;  $\rho$  is the specific mass ( $kg/m^3$ ),  $c$  is the specific heat ( $J/kg K$ ) of the material

e  $G$  is the rate of internal heat generation (internal energy) per unit volume ( $W/m^3$ ). For an isotropic material in which the thermal coefficients  $k$ ,  $\rho$  and  $c$  are all constant, and there is no internal heat generation and Equation (1) can be rewritten as:

$$\nabla^2 T = \frac{1}{\alpha} \frac{\partial T}{\partial t}, \quad (2)$$

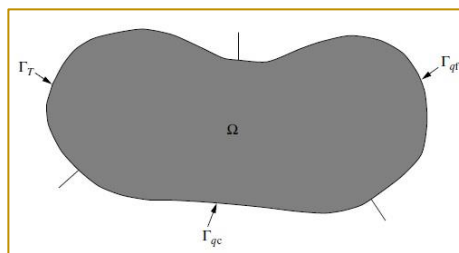
where  $\nabla^2$  is the Laplacian operator, and  $\alpha = \frac{k}{\rho c}$ , is called thermal diffusivity ( $m^2/s$ ) (see e.g. [LEWIS et al. 2004]).

### 2.1.1. INITIAL AND BOUNDARY CONDITIONS

The solution of Equation (1) is possible if the defined initial and boundary conditions are

appropriate to the analyzed physical problem. Consider an arbitrary domain over which the equation of heat conduction applies, bounded by a surface, such that, where is the surface on which a temperature  $T$  function is prescribed, and are the areas in which affect heat flow from, for example, by an external heat source and convective heat flow, respectively (see Figure 2).

Figure 2. Boundary conditions.



According to [Lewis et al. 2004], the boundary conditions for the heat equation can be of two types, or a combination thereof - of Dirichlet condition, which is the set temperature in a

portion of the domain boundary and/or Neumann condition, which is flow heat prescribed in another portion of the domain boundary.

Dirichlet Condition

$$T = T_0, \text{ in } \Gamma_T. \quad (3)$$

Neumann Condition

$$q = -k \frac{\partial T}{\partial n}, \text{ in } \Gamma_{qf}, \quad (4)$$

where  $T_0$  is a prescribed temperature ( $K$ ),  $n$  is the normal vector to the surface  $\Gamma_{qf}$  and  $q$  is the steady flow ( $W/m^2$ ).

The convective heat flux also fits as a Neumann boundary condition and can be written as:

$$-k \frac{\partial T}{\partial n} = h(T - T_a), \text{ in } \Gamma_{qc}, \quad (5)$$

where  $h$  is the heat transfer coefficient by convection ( $W/m^2$ ),  $T$  is the surface temperature in  $\Gamma_{qc}$  and  $T_a$  is the temperature of the adjacent fluid. The initial condition is the

temperature all the domain  $\Omega$  in a reference time  $t = t_0$ , usually called initial instant. This temperature can be represented as:

$$T = T_0, \text{ in } \Omega \text{ in } t = t_0. \quad (6)$$

The Equations (4) and (5) can be described in terms of the cosine directors of the normal

vector  $n = \{\tilde{l}, \tilde{m}, \tilde{n}\}$ , appropriate to the surface  $\Gamma_{af}$  and  $\Gamma_{qc}$  :

$$k_x(T) \frac{\partial T}{\partial x} \tilde{l} + k_y(T) \frac{\partial T}{\partial y} \tilde{m} + k_z(T) \frac{\partial T}{\partial z} \tilde{n} = q, \quad (7)$$

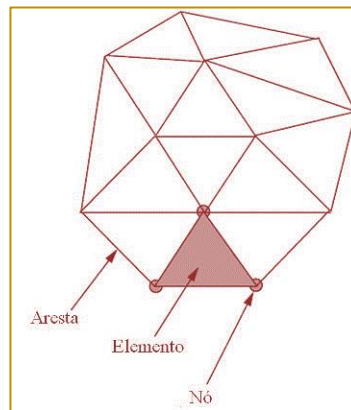
$$k_x(T) \frac{\partial T}{\partial x} \tilde{l} + k_y(T) \frac{\partial T}{\partial y} \tilde{m} + k_z(T) \frac{\partial T}{\partial z} \tilde{n} = h(T - T_a). \quad (8)$$

## 2.2. THE FINITE ELEMENT METHOD

The FEM is a methodology to obtain numerical solution of equations in differential and integral form, particularly in physical-mathematical field equations. These are approximate to single domain regions (triangles, quadrilaterals, tetrahedra, etc.) to meet together, the continuity of the field variables (displacement, temperature, pressure) at nodal points of elements of the domain (see e.g. [Gupta and Meek 1996]).

According to [Krüger 2001], in problems of Continuum Mechanics, functions as displacements, stresses, pressures and temperature are associated with infinite points of the solution region. The process of discretization in finite elements reduces the size of the problem to a finite number of unknowns by dividing the solution domain elements (mesh) and expressing the variables in terms of approximation of functions on each element. Figure 3 shows an example of a mesh of finite elements.

Figure 3. Example of finite element mesh.



Source: Adapted from [Lewis et al. 2004].

The steps to achieve an approximate solution to a physical model using FEM (according to [Lewis et al. 2004]) are:

- 1- Discretization of continuous: dividing the solution region into subdomains or non-overlapping elements;
- 2- Selection of basis functions or interpolation: such functions determine the variation of the unknown variable in study;

3- Formulation of the equations of nodes: take into account the individual properties of each element;

4- Assembling the global matrix for simultaneous solution of the elements equations;

5- Application of the initial and boundary conditions and loadings;

6- Resolution of the global system for determining the nodal results, such displacements and temperatures on different nodes.

There are several approaches to formulate problems in finite element, such as Direct Method, Minimum Potential Energy, Variational methods and Waste weighted. In the following, Equation (1) is discretized by a

method of the latter case, the Galerkin method.

### 2.2.1 GALERKIN METHOD

An expression that describes how temperatures are interpolated in a finite element is given by the following equation:

$$T(x, y, z, t) = \sum_{i=1}^n N_i(x, y, z) T_i(t), \quad (9)$$

where  $N_i$  are the basis functions,  $n$  is the number of nodes in an element and  $T_i(t)$  is a nodal temperature time-dependent.

The most widely used basic functions are polynomial type, in particular linear and quadratic according to the size of the mesh elements. Examples of such functions and

applications can be viewed in [Lewis et al. 2004] and [Onate 2009].

Multiplying Equation (1) a base function  $N_i$  and integrating over the domain of analysis, the representation of Galerkin is:

$$\int_{\Omega} N_i \left[ \frac{\partial}{\partial x} \left( k_x(T) \frac{\partial T}{\partial x} \right) + \frac{\partial}{\partial y} \left( k_y(T) \frac{\partial T}{\partial y} \right) + \frac{\partial}{\partial z} \left( k_z(T) \frac{\partial T}{\partial z} \right) + G - \rho c \frac{\partial T}{\partial t} \right] d\Omega = 0. \quad (10)$$

Using integration by parts on the first three terms of Equation (10) we obtain:

$$\begin{aligned} & - \int_{\Omega} \left[ k_x(T) \frac{\partial N_i}{\partial x} \frac{\partial T}{\partial x} + k_y(T) \frac{\partial N_i}{\partial y} \frac{\partial T}{\partial y} + k_z(T) \frac{\partial N_i}{\partial z} \frac{\partial T}{\partial z} \right] d\Omega + \int_{\Omega} \left[ N_i G - N_i \rho c \frac{\partial T}{\partial t} \right] d\Omega \\ & + \int_{\Gamma_q} N_i k_x(T) \frac{\partial T}{\partial x} \tilde{l} d\Gamma_q + \int_{\Gamma_q} N_i k_y(T) \frac{\partial T}{\partial y} \tilde{m} d\Gamma_q + \int_{\Gamma_q} N_i k_z(T) \frac{\partial T}{\partial z} \tilde{n} d\Gamma_q = 0, \end{aligned} \quad (11)$$

where  $\Gamma_q = \Gamma_{qc} \cup \Gamma_{qf}$  and in  $\Gamma_T$  the temperature variation is zero when considering that this boundary the

temperature is constant. Note that Equations (7) e (8),

$$\int_{\Gamma_q} N_i k_x(T) \frac{\partial T}{\partial x} \tilde{l} d\Gamma_q + \int_{\Gamma_q} N_i k_y(T) \frac{\partial T}{\partial y} \tilde{m} d\Gamma_q + \int_{\Gamma_q} N_i k_z(T) \frac{\partial T}{\partial z} \tilde{n} d\Gamma_q = - \int_{\Gamma_{qf}} N_i q d\Gamma_{qf} - \int_{\Gamma_{qc}} N_i h(T - T_a) d\Gamma_{qc}. \quad (12)$$

Through Equation (12) and approach (9), the Equation (11) can be written as:

$$\begin{aligned} & - \sum_{j=1}^n \int_{\Omega} \left[ k_x(T) \frac{\partial N_i}{\partial x} \frac{\partial N_j}{\partial x} T_j(t) + k_y(T) \frac{\partial N_i}{\partial y} \frac{\partial N_j}{\partial y} T_j(t) + k_z(T) \frac{\partial N_i}{\partial z} \frac{\partial N_j}{\partial z} T_j(t) \right] d\Omega \\ & + \int_{\Omega} \left[ N_i G - N_i \rho c \sum_{j=1}^n N_j \frac{\partial T_j(t)}{\partial t} \right] d\Omega - \int_{\Gamma_{qf}} N_i q d\Gamma_{qf} - \int_{\Gamma_{qc}} N_i h \left( \sum_{j=1}^n N_j T_j(t) - T_a \right) d\Gamma_{qc} = 0, \end{aligned} \quad (13)$$

where  $i$  and  $j$  represents nodes. Is possible to write in matrix terms Equation (13):

$$[C_{ij}] \left\{ \frac{\partial T_j}{\partial t} \right\} + [K_{ij}] \{T_j\} = \{f_i\}, \tag{14}$$

where the term  $\frac{\partial T_j}{\partial t}$  can be discretized using the finite difference method, as can be seen in

[Lewis et al. 2004] and the other terms of the Equation (14) are defined as:

$$[C_{ij}] = \int_{\Omega} \rho c N_i N_j d\Omega,$$

$$[K_{ij}] = \int_{\Omega} \left[ k_x(T) \frac{\partial N_i}{\partial x} \frac{\partial N_j}{\partial x} + k_y(T) \frac{\partial N_i}{\partial y} \frac{\partial N_j}{\partial y} + k_z(T) \frac{\partial N_i}{\partial z} \frac{\partial N_j}{\partial z} \right] d\Omega + \int_{\Gamma_{qc}} h N_i N_j d\Gamma_{qc} \text{ and}$$

$$\{f_i\} = \int_{\Omega} N_i G d\Omega - \int_{\Gamma_{qf}} q N_i d\Gamma_{qf} + \int_{\Gamma_{qc}} h T_a N_i d\Gamma_{qc}.$$

### 2.3. ARIMA MODELS

The Auto-Regressive Integrated Moving Average (ARIMA) models, developed by [Box and Jenkins 1970], are widely known and used in modeling and forecasting time series. Let  $y_t (t = 1, \dots, T)$  be a time series, i.e., a set of

observations ordered in time, displaying an auto-correlation structure. According to [Liu 2009],  $y_t (t = 1, \dots, T)$  can be seen as a realization of a stochastic ARIMA  $(p, d, q)$  process, if it can be represented by

$$\nabla^d y_t = \phi_0 + \sum_{j=1}^p \phi_j \nabla^d y_{t-j} + \sum_{i=1}^q \theta_i e_{t-i} + e_t, \tag{15}$$

where  $\nabla^d := (I - B)^d$  is the difference operator, with  $d$  representing its order, and  $B$  is the delay operator, defined as  $B^k y_t := y_{t-k}$ , with  $k$  belonging to a set of integers;  $(\phi_i)_{i=0}^p$  and  $(\theta_i)_{i=0}^q$  are the sets of auto-regressive and moving average parameters, respectively, such that  $\phi_p \neq 0$  and  $\theta_q \neq 0$ , both satisfying the invertibility and the stationarity conditions (as in [Hamilton 1994]);  $e_t$  represents a state of the random variable  $\varepsilon_t (t = 1, \dots, T)$ , a stochastic white noise process, which mean and auto-covariance are stationary at zero;  $p$  and  $q$  are, respectively, the orders of the auto-regressive component, denoted by  $\sum_{j=1}^p \phi_j \nabla^d y_{t-j}$ , and the moving average component, represented by  $\sum_{i=1}^q \theta_i e_{t-i}$  in Equation (15).

plausible values for the parameters  $p$ ,  $d$ , and  $q$ , in Equation (15), which can often sometimes be obtained by profile analysis of simple autocorrelation functions and partial waste (as in [Hamilton 1994]); (ii) define the method to be used to estimate the ARIMA parameters (the most commonly used is the maximum likelihood estimation method); and, (iii) perform a diagnostic test to choose the most parsimonious and appropriate model to be used to generate both the in-sample and out-of-sample forecasts of the underlying time series  $y_t (t = 1, \dots, T)$ .

### 3. THE PROPOSED METHOD AND ITS APPLICATION TO THE ITAIPU DAM

A buttress dam block of the IHPP dam, located on the Paraná River on the border between Brazil and Paraguay, was used in the application of the proposed method to predict the temperature field in this block. Four thermometers were installed in the block's surface and their measurements of monthly temperature recorded over a period of four years from 2010 to 2014. Figure 4 shows the

According to [Liu 2009], in order to obtain the best possible ARIMA model, the following three basic steps should be taken: (i) obtain

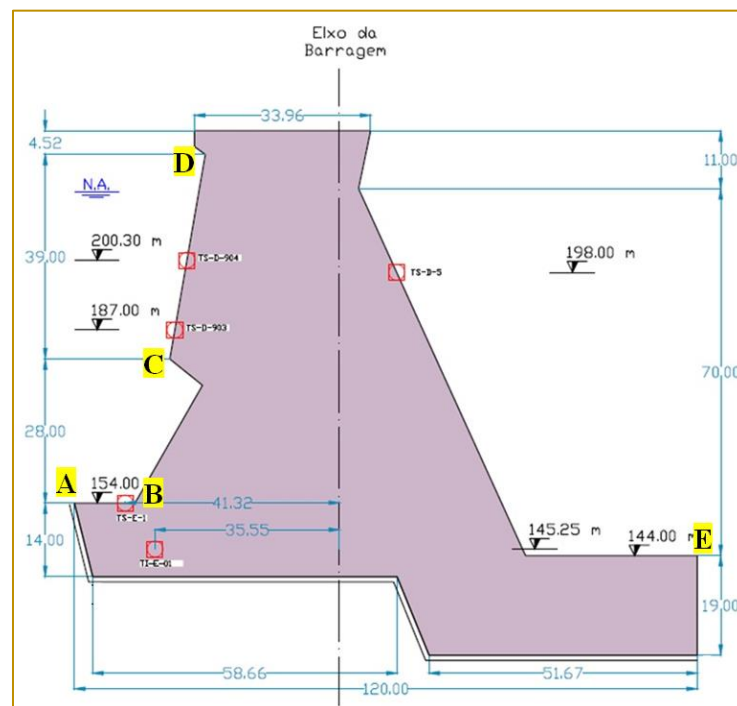
two-dimensional geometry of the block and the location of thermometers: TS-D-903, TS-D-904, TS-E-1 and TS-D-5.

Monthly temperatures for each thermometer were collected and used in the application. The data was split into a training in-sample (from 11/01/2010 to 11/11/2013) and a forecasting out-of-sample (from 09/12/2013 to 27/11/2014).

The method consists of two parts. One part deals with the statistical forecasting of temperature while the other with the heat conduction model for the concrete block. The initial stage consists in disaggregating the monthly data into daily estimations with

polynomial interpolation using cubic splines (with a MATLAB program). So, cubic splines interpolating curves were fitted to the data of each of the thermometers to approximate data daily temperatures, as the readings of thermometers in the study period were only monthly, in order that it is possible later to obtain the thermal model solution of the block. The simplicity of representation and facility the splines can be computed, cause they are popular in the data set in computer science and computer engineering, predominantly in computer graphics. The term spline is a device used by shipbuilders to draw soft forms.

Figure 4. Geometry buttress block, location of thermometers and delimitation of boundary conditions.



According to [Ruggiero and Lopes 1997], a cubic spline interpolation can be defined as follows: Let  $f(x)$  be a function defined at the points  $x_0 < x_1 < \dots < x_n$ , the function  $S_3(x)$  is

called *cubic spline* with nodes at the points  $x_i$ ,  $i = 0, \dots, n$  if it satisfies the following conditions:

I - In each subinterval  $[x_i, x_{i+1}]$ ,  $i = 0, \dots, (n-1)$ ,  $S_3(x)$  is a polynomial of degree 3:  $s_3(x)$ ;

II -  $S_3(x)$  is continuous and has continuous derivatives of the second order  $[x_0, x_n]$ ;

$$III - S_3(x_i) = f(x_i), i = 0, \dots, n.$$

This is followed by fitting an ARIMA model to each of the four daily series adjusted by splines in the training in-sample (November 2010 to October 2013) and producing out-of-sample forecasts (November 2013 to October 2014) (with an EViews program).

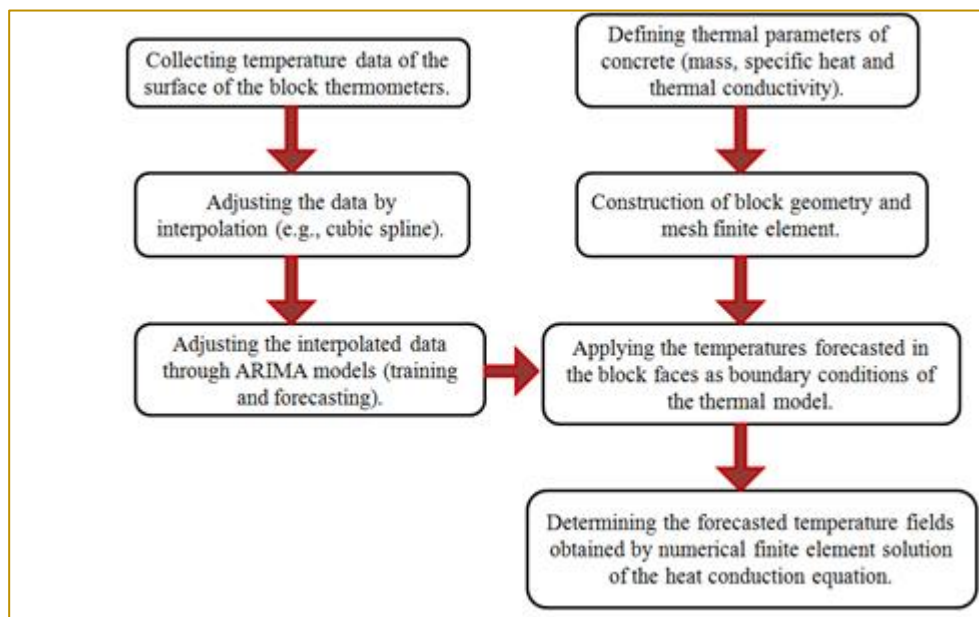
The heat conduction model part on the other hand starts by defining the concrete thermal parameters (specific mass and heat and thermal conductivity), block geometry and the mesh of finite elements (with an ANSYS program). The forecasts from the ARIMA models are then applied to the geometry contour and used to solve the heat conduction models via FEM (also with ANSYS).

After obtaining the monthly temperatures expected for a period of one year, these were taken as boundary conditions in the following block: when viewing Figure 5, from point A to

point B (clockwise) the adopted temperature function was the thermometer TS E-1, from point B to C of TS-D-903 thermometer, point C to D TS-D-904 thermometer from the point D to E TS-D-5 thermometer and finally from point D to point E, the face was considered that it had zero heat flow, ie,  $q = 0$ .

With the well-defined boundary conditions, heat conduction equation (1) can be solved by applying the FEM and the prediction of transient temperature field in the block is checked. The thermal properties of concrete, initial condition to be adopted in the thermal model, the necessary simplifications and the results obtained from the FEM are discussed in the following subsection. The Figure 5 shows a flowchart of those stages of the proposed method.

Figure 5. Flowchart of the proposed method.



### 3.1 NUMERICAL RESULTS

The Figure 6 shows for each of the four series of temperature, comparative graphs between the temperatures estimated by the cubic splines and those forecast by the ARIMA

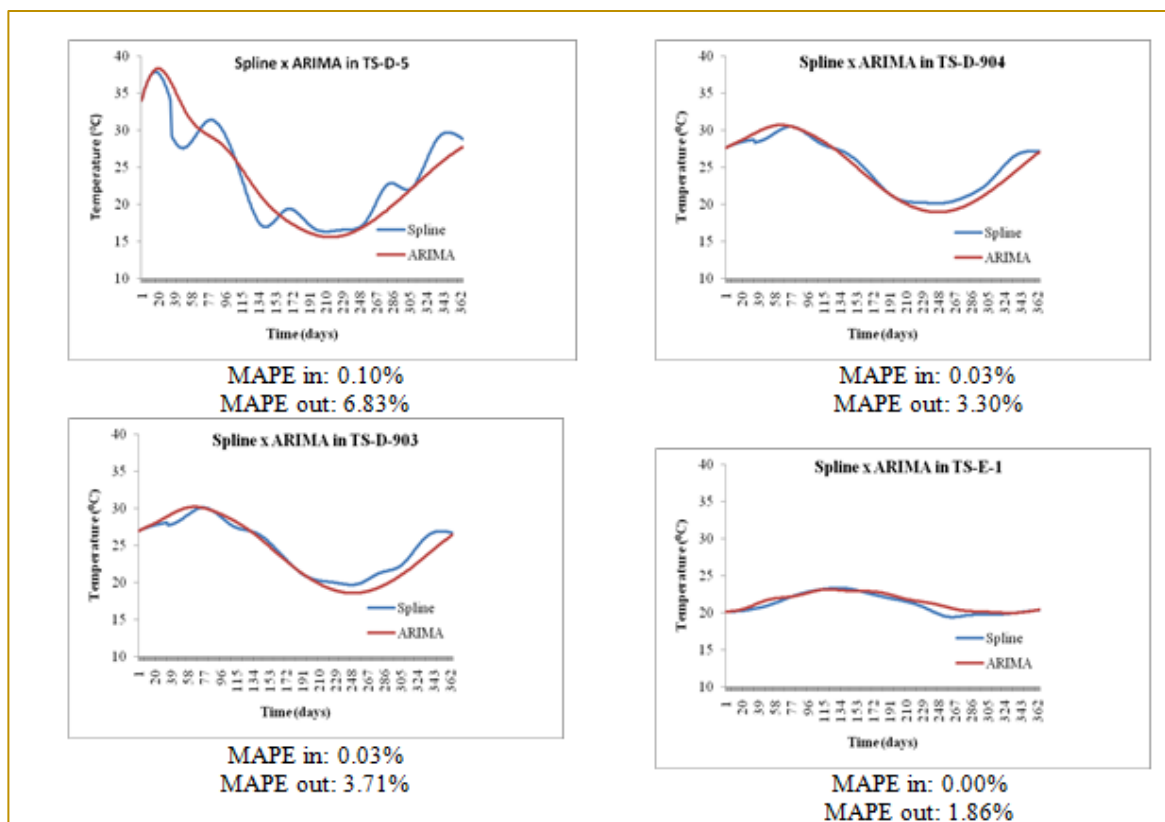
models for the out-of-sample year. The MAPE (Mean Absolute Error Percentage) was used to estimate the error between the models, and it is given by the following expression:

$$\text{MAPE} = \frac{\sum_{i=1}^n \left| \frac{T_i - \hat{T}_i}{T_i} \right|}{n}, \quad (166)$$

where  $n$  is the number of observed data,  $T_i$  the  $i$ -th temperature estimated by the cubic splines and  $\hat{T}_i$  the approximate value of the  $i$ -th temperature determined by the ARIMA

model. The MAPE *in* is the MAPE calculated for the in-sample period and MAPE *out* is calculated for the out-of-sample period for each of the 4 surface thermometers.

Figure 6. Cubic splines vs ARIMA for the out-of-sample period for each of the surface thermometers (TS-D-5, D-TS-903, TS-904 and TS-D-E-1).



Note from the plots in Figure 6 and the respective low MAPE in values that the forecasts by the ARIMA models are approximating well the data interpolated by cubic splines.

Some simplifications were considered in the process of generating the numerical thermal model: no source of heat, the material homogeneity, isotropic and linear elastic behavior, considered the state of plane stress and simplifications in geometric section (chamfers, drainage, supports, and other beams). The following values of thermal properties of concrete were used in the

model: a thermal conductivity of  $1.2W(mK)^{-1}$ , a specific heat of  $895.38J(kg K)^{-1}$  and a specific mass of  $2550kgm^{-3}$ .

The simulations performed in ANSYS environment - Workbench V16.1 and graphics in Thermal Transient environment. The scheme accomplished through software to block thermal analysis started with the geometry of the mesh creation, definition of the boundary conditions and the thermal properties of concrete. Initially a stationary thermal analysis was carried out in order to create a temperature field and entered in the

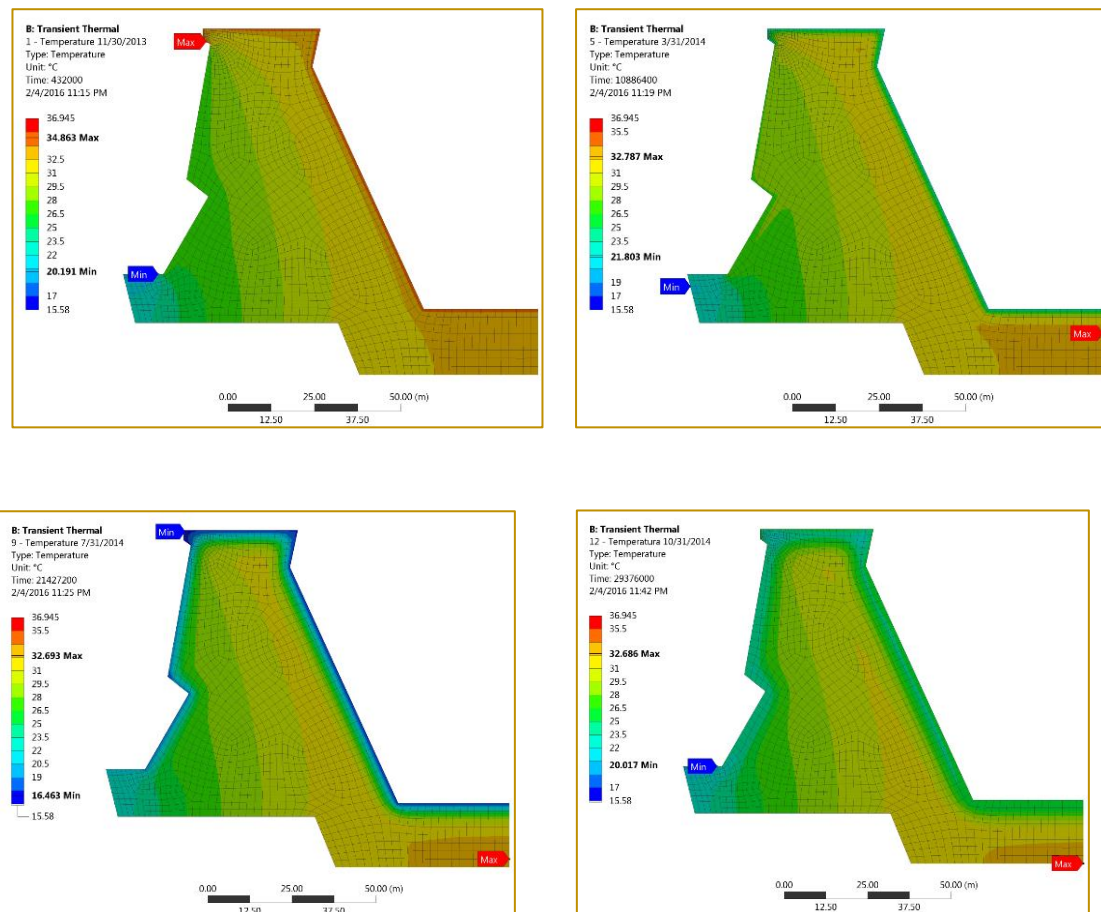
transient thermal analysis as an initial condition. Finally, monthly temperature fields were generated throughout the out-of-sample forecasting year.

The mesh used for the geometry shown in Figure 7 showed 1386 elements (SHELL 131 type, which is a shell element with four nodes and the temperature up to 32 degrees of freedom at each node and such element served for transient analyzes and stationary) and 1497 nodes, so that almost entirely the elements are quadrangular and some triangular. After the geometry of the mesh and concrete properties are defined, a stationary simulation with the temperature data

approximate temperature on 25/11/2013 was performed with the aim being to block an equilibrium temperature range and this used as initial temperature of the block to the transient analysis.

Following temperature data set of 4 thermometers obtained through the ARIMA model in the period from 26/11/2013 to 31/10/2014 served as boundary conditions to the thermal model, as mentioned earlier in this chapter. This was solved by FEM in ANSYS. Figure 7 provides trimonthly temperature fields during this period, considering the last day of the month.

Figure 7. Trimonthly transient temperature fields.



The color scale at the left hand side of each of the four diagrams in Figure 7 shows the various temperatures (in Celsius) in increasing order from minimum values at the bottom (dark blue) to maximum values at the top (red). Looking at the block in each diagram, note that the highest temperatures are in the downstream phase (contact with the environment), while warmer temperatures are located upstream (contact with the reservoir).

The simulation results as displayed in Figure 7 showed that heat storage in the dam of the soul throughout the year, since the color change in the graph is closest to the surface, and as was to be expected on the type of material, the energy dissipation is gradually slow. Moreover, it has monitored a control point within the structure where the internal thermometer TI-E-01 is located (see Figure 4). The data measured by this thermometer for

the out-of-sample forecasting year were compared with those obtained by numerical simulation (the FEM) and the calculated MAPE was 15.37%. With this, the thermal model of the block is within the engineering safety limits, according to the superintendence of the Itaipu Power Plant Engineering.

#### 4. CONCLUSIONS

Predicted temperature fields provided by ARIMA forecasting models and the finite element method for heat equation solution were determined for a case study on a buttress dam block of Itaipu Hydroelectric Power Plant. Observed data of four surface thermometers in the block have been adjusted by interpolating cubic splines functions and their ARIMA forecasting models determined.

The daily forecasts obtained one year ahead for each of the thermometers were used as boundary conditions for solving the heat

conduction equation for the concrete block. The numerical solution of the heat conduction equation was achieved through the Finite Element Method. To validate the method, the real temperatures for the forecast period on a test point, which is located an internal thermometer (TI-E-1), were compared with those obtained with the values obtained by FEM, reaching a MAPE satisfactory.

The proposed method in this paper is a novel approach to modelling heat transfer by conduction in concrete dam. One year ahead temperature field predictions in concrete dam blocks have been shown feasible in this study. Another benefit of this methodology is the fact that it encourages further studies to investigate the prediction of stresses and strains in the thermal source structure that is essential for preventive measures in relation to the life of the structure.

#### REFERENCES

- [1] Box, George and Jenkins, Gwilym (1970). *Time Series Analysis: Forecasting and Control*. San Francisco: Holden-Day.
- [2] Daoud, M., Galanis, N., and Balliiv, G. (1997). Calculation of the Periodic Temperature Field in a Concrete Dam. *Canadian Journal of Civil Engineering*, 24(5), 772–784.
- [3] Gupta, K. K., and Meek, J. L. (1996). A Brief History of the Beginning of the Finite Element Method. *International Journal for Numerical Methods in Engineering*, 39, 3761–3774.
- [4] Hamilton, J. (1994). *Time Series Analysis*. Princeton University Press.
- [5] Krüger, D. A. V. (2001). *Análise Térmica Transiente de Estruturas de Concreto Executadas por Camadas*. UFPR.
- [6] Lewis, R. W., Nithiarasu, P., and Seetharamu, K. N. (2004). *Fundamentals of the Finite Element Method for Heat and Fluid Flow*. John Wiley & Sons.
- [7] Liu, L.-M. (2009). *Time Series Analysis and Forecasting*. Scientific Computing Associates Corp.; 2nd Edition edition.
- [8] Madenci, E., & Guven, I. (2015). *The Finite Element Method and Applications in Engineering Using ANSYS*. 2. ed., Springer Science & Business Media.
- [9] Maken, D. D., Léger, P., and Roth, S. N. (2013). Seasonal thermal cracking of concrete dams in northern regions. *Journal of Performance of Constructed Facilities*, American Society of Civil Engineers.
- [10] Mirzabozorg, H., Hariri-Ardebili, M. A., Shirkhan, M., and Seyed-Kolbadi, S. M. (2014). Mathematical Modeling and Numerical Analysis of Thermal Distribution in Arch Dams Considering Solar Radiation Effect. *The Scientific World Journal*, Hindawi Publishing Corporation.
- [11] Moaveni, S. (2008). *Finite Element Analysis: Theory and Application with ANSYS*. 3. ed., Pearson Education India.
- [12] Noorzaei, J., Bayagoob, K. H., Thanoon, W. A., and Jaafar, M. S. (2006). Thermal and Stress Analysis of Kinta RCC Dam. *Engineering Structures*, Elsevier, 28(13), 1795–1802.
- [13] Onate, E. (2009). *Structural Analysis with the Finite Element Method. Linear Statics: Basis and Solids*. Springer Science & Business Media, Vol. 1.
- [14] Ozisik, M. N. (1993). *Heat Conduction*. John Wiley & Sons.
- [15] Ruggiero, M. A. G., and Lopes, V. L. R. (1997). *Cálculo Numérico: Aspectos Teóricos e Computacionais*. 2. ed., Makron Books do Brasil.